Prevention of Peptide Fibril Formation in an Aqueous Environment by Mutation of a Single Residue to Aib†

Janet R. Kumita,‡ Chris J. Weston,§ Lin-P'ing Choo-Smith,|| G. Andrew Woolley,‡ and Oliver S. Smart*,§

Department of Chemistry, University of Toronto, 80 Saint George Street, Toronto, Ontario, M5S 3H6, Canada, School of Biosciences, University of Birmingham, Edgbaston, Birmingham B15 2TT, United Kingdom, and Institute for Biodiagnostics, National Research Council of Canada, 435 Ellice Avenue, Winnipeg, MB, R3B 1Y6 Canada

Received September 15, 2002; Revised Manuscript Received December 24, 2002

ABSTRACT: The behavior of a number of 16 residue polypeptides with a sequence Acetyl-EAC-AR***XZ***AACEAAARQ-amide, where ***X*** = V or A and ***Z*** = A or Aib, is studied under aqueous conditions. It is shown that the substitution of a single alanine residue by α-aminoisobutyric acid (Aib) completely alters both the conformation and the aggregation properties of the peptides. The Ala-Ala (***X***,***Z*** = A,A) peptide is shown by circular dichroism and FTIR methods to adopt a predominately *β*-sheet conformation. Furthermore, the peptide has limited solubility and is shown to form fibrils by electron microscopy and thioflavin T binding assays. In contrast, a single substitution at the center of peptide of alanine to Aib (***X***,***Z*** = A,Aib) completely abolishes fibril formation and alters the conformation to a mixture of random coil and α-helix. The results show that Aib is a strong *β*-sheet disrupter that is also able to adopt a helical conformation. This is linked to its role in peptaibol antibiotics. Aib provides an attractive alternative to proline and other substitutions in producing peptide variants with a lower tendency to produce fibril aggregates.

A large number of human diseases, including Alzheimer's and Creutzfeldt−Jakob disease, appear to result from aberrant protein folding and subsequent aggregation (*1*, *2*). Recent work has highlighted the toxicity of early intermediates in aggregation pathways and has suggested that even normally nontoxic proteins can become lethal under specific conditions (*3*, *4*). Strategies for controlling the likelihood of such potentially harmful conformations are consequently of substantial interest.

It is clear that the backbone conformation (e.g., *β*-sheet vs α-helix, or random-coil) plays a central role in determining the aggregation propensity of protein segments (*5*). In general, sequences with a preference for adopting *β*-sheet conformations are more likely to show aggregation than those preferring helical secondary structures (*5*, *6*). A number of workers have reported some success in preventing amyloid formation by prion proteins and Alzheimer's A*β* peptides using synthetic peptides, termed *β*-sheet breakers (*7*, *8*). These synthetic peptides contain proline residues (*7*−*9*), D-amino acids (*7*, *10*), or *N*-methylated amino acids (*11*). All of these modifications interfere with the ability of the peptide to adopt, or for *N*-methyl amino acids (*12*), to propagate *β*-sheet conformations. Furthermore, when added in excess the modified peptides can induce breakdown of the aggregated *β*-sheet structure of the wild-type peptide (*7*, *8*, *11*). This strategy may provide a route to produce useful therapeutics (*8*), although caution should be observed as natural racemization of amino acids in *β*-amyloid peptide has been linked to toxicity (*10*).

The nonnatural amino acid Aib,[1] found in peptaibol antibiotics such as alamethicin, emerimicins, and suzukacillin (*13*, *14*), is a well-known helix stabilizer (*15*−*17*). Aib differs from alanine in that the hydrogen atom normally attached to the α carbon is replaced by a methyl group. Aib has been demonstrated to disrupt *β*-sheets in organic solvents and in the solid state. Moretto et al. (*18*) and Narita et al. (*19*) studied the effects of Aib on oligo-valine and oligo-leucine peptides and found that the *β*-sheet disrupting ability of Aib was greater than that of proline (*18*). The effects of Aib were found to be solvent-dependent but because of the hydrophobic nature of these peptides, examination of their conformational behavior in water was not possible (*18*, *19*).

In this paper, we report the effects of Aib on the conformational behavior of a set of peptides in aqueous solutions. Single Ala to Aib substitutions were found to result in secondary structure changes from *β*-sheet to α-helix/random-coil equilibria. This conformational control of backbone structure is shown to prevent fibril formation and dramatically alters the aqueous solubility of the peptides.

MATERIALS AND METHODS

Peptide Synthesis. Standard fluorenylmethoxycarbonyl-based solid-phase peptide synthesis methods were used to

† We would like to acknowledge NSERC (Canada) (G.A.W.) and the BBSRC (UK) grant B/16000 (O.S.S.) for financial support. J.R.K. was supported by an NSERC studentship.

* Corresponding author. E-mail: o.s.smart@bham.ac.uk. Telephone: +44 121 414 4090. Fax: +44 121 414 5925.

‡ University of Toronto.

§ University of Birmingham.

|| National Research Council of Canada.

[1] Abbreviations: Aib, α-aminoisobutyric acid; ANS, 8-anilino-1-naphthalene sulfonic acid; CD, circular dichroism; DTT, dithiothreitol; EM, electron microscopy; FTIR, Fourier transform infrared; MES, 2-(*N*-morpholino)-ethanesulfonic acid; Thio-T, thioflavin T.

10.1021/bi026856t CCC: $25.00
Published on Web 03/28/2003

prepare all peptides. Peptides were constructed on Pal-resin (capacity 0.55 mmol/g) (Advanced ChemTech, Louisville KY). Coupling used 3 equiv of HATU [*O*-(7-azobenzotriazol-1-yl)-1,1,3,3-tetramethyluronium hexafluorophosphate] (Sigma-Aldrich, Canada), 6 equiv of DIPEA (*N*,*N*-diisopropylethylamine), and 3 equiv of amino acid (Novabiochem, San Diego, CA). Aib-F was synthesized following the procedure of Kaduk and co-workers (*20*). Peptides were purified by HPLC (Apex Presil C18 8 μm column (Jones Chromatography, Lakewood, CO)) using a linear gradient from 0 to 80% acetonitrile/H_2O (+0.1% trifluoroacetic acid) over 45 min. The peptide primary structures were confirmed by electrospray ionization MS and amino acid analysis (HSC Biotechnology Service Centre, Toronto); JRK-{AlaAla} (observed 1604 Da; calculated ($C_{62}H_{106}N_{24}O_{22}S_2$): 1603.8 Da); JRK-{AlaAib} (observed 1617 Da; calculated ($C_{63}H_{108}N_{24}O_{22}S_2$): 1617.8 Da); JRK-{ValAla} (observed 1631 Da; calculated ($C_{64}H_{110}N_{24}O_{22}S_2$): 1631.9 Da); and JRK-{ValAib} (observed 1646 Da; calculated ($C_{65}H_{112}N_{24}O_{22}S_2$): 1645.9 Da). The purity by HPLC was >90%.

Circular Dichroism Measurements. CD measurements were performed with a Jasco Model J-710 spectropolarimeter. All measurements were made in a thermostated quartz cuvette (0.1-cm path length). Temperatures were measured using a microprobe directly in the sample cell. All samples were dissolved in 5 mM phosphate buffer (pH 7). DTT (3 mM) was present in the peptide samples to ensure that cysteine residues were in the reduced form. Spectra reported are averages of three individual experiments of five scans each, with the appropriate background spectrum subtracted unless otherwise reported. A scan speed of 10 nm/min, with a 0.5-nm bandwidth and a 4-s response time was used.

FTIR Measurements. Sample preparation involved suspending the lypohilized peptide in ^2H_2O (Sigma, St. Louis, MO) to a final concentration of 10 mg/mL in 1.7 mM phosphate buffer (pD = 7) and 1 mM DTT. For the acquisition of FTIR spectra, 5 μL of the peptide solution was placed between a pair of CaF_2 windows separated by a 50 μm Teflon spacer and mounted in a Harrick demountable cell. For each spectrum, 512 interferograms were collected on a BioRad FTS-40A FTIR spectrometer and Fourier transformed to generate a spectrum with 2 cm^{-1} resolution. A ^2H_2O buffer spectrum containing DTT was recorded under identical conditions and subtracted from the peptide spectra. Weak residual absorptions arising from water vapor were interactively subtracted. Fourier self-deconvolution was carried out as previously described (*21*) using a halfwidth of 13.5 and a resolution enhancement factor $k = 1.75$.

Molecular Modeling. All modeling work was performed using the SYBYL package (Tripos) on a Silicon Graphics Octane2 workstation. The peptide JRK-{ValAla} was modeled as an extended β-strand with main chain dihedrals $\phi = -119°$, $\psi = +113°$ characteristic of a parallel β-sheet (*22*). Optimal packing between adjacent strands and salt bridge formation was achieved by energy minimization using the AMBER96 force field (*23*). Pictures of the final model were produced using the Molscript program (*24*).

Electron Microscopy. Peptides were prepared at a concentration of 0.3 mg/mL in 5 mM phosphate buffer, pH 7, with 3 mM DTT. Concentrations were checked by amino acid analysis (Alta Biosciences). After maturation of at least 3 days at 20 °C, a small (~10 μL) aliquot of the solution was pipetted onto Formvar-coated 200-mesh copper grids. After 2 min, solvent was removed by blotting with filter paper, and 2% w/v uranyl acetate was used to stain the sample for 4 min. Grids were then blotted again and air-dried before analysis using a JEOL 1200EX microscope operating at 80 kV with 40k magnification. Images were obtained by exposing the film for 1 s.

Dye Binding Assays. The peptide samples used for electron microscopy were also used for Thio-T and ANS dye binding assays. All spectra were recorded on a Perkin-Elmer LS50B fluorimeter at room temperature. The protocols used were adapted from Smith and Radford (*25*). For ANS binding, a 250 μM solution of ANS was used in a buffer containing 25 mM Tris-HCl, 25 mM sodium acetate, 25 mM glycine, and 25 mM MES titrated to pH 7 (*25*). A 60-μL aliquot of the (0.3 mg/mL) peptide was added to 3 mL of this solution in a 10-mm square fluorescence cuvette. ANS binding was determined immediately by recording the fluorescence emission spectra, both in the absence and in the presence of peptides, using an excitation wavelength of 389 nm (5-nm slit widths, 20 scans).

To obtain spectra demonstrating Thio-T binding, a 10 μM solution of the dye was used in a 50 mM Tris-HCl buffer titrated to pH 8.5. To 3 mL of this solution, a 60-μL aliquot of the peptide (0.3 mg/mL) was added. Emission spectra were recorded immediately using an excitation wavelength of 444 nm (*25*) with 5-nm slit widths (20 scans).

Time-Resolved Studies. For time-resolved studies, a 0.3 mg/mL (~180 μM) solution of JRK-{AlaAla} was prepared in 5 mM phosphate buffer, pH 7, containing 3 mM DTT, using sonication to ensure rapid solubilization. A quantity of this solution was diluted 12-fold immediately (to ~15 μM) in an identical buffer, and the two samples were left to age at 20 °C. The CD signal of the ~15 μM sample was followed immediately at 220 nm in a JASCO Model J-810 spectropolarimeter running in time course mode, with a 1-mm path length at 20 °C (1-nm bandwidth, 1-s response, 1-h time course). A steady baseline was obtained prior to the introduction of the sample into the cell holder.

The rate of fibril formation was assayed for the two samples by Thio-T binding, adapting the procedure set out above. To allow direct comparison of the Thio-T binding for the two different concentrations, aliquots were adjusted so an identical amount of peptide was added in each case. Either 360 μL for the dilute (~15 μM) peptide sample or 30 μL for the concentrated sample together with 330 μL of the phosphate buffer was added to 2.8 mL of 10 μM solution of the dye. Emission spectra were recorded as above, and the fluorescence intensity of the peak at 485 nm was recorded.

RESULTS

Two pairs of peptides -JRK-{AlaAla}/ JRK-{AlaAib} and JRK-{ValAla}/JRK-{ValAib} were synthesized and purified by HPLC. The primary sequences are shown in Figure 1. These sequences were chosen based on previous work by Baldwin, Stellwagen, and colleagues who found that peptides of general sequence Ac-A(EAAAR)$_3$ adopt stable monomeric helical structures at low temperatures in water (*26*−*28*). We

JRK{AlaAla}
Ac-EACARAAAACEAAARQ-NH_2

JRK{AlaAib}
Ac-EACARA**Aib**AACEAAARQ-NH_2

JRK{ValAla}
Ac-EACARVAAACEAAARQ-NH_2

JRK{ValAib}
Ac-EACARV**Aib**AACEAAARQ-NH_2

FIGURE 1: Primary sequences of the peptides studied.

introduced Val, Aib, and Cys residues into these sequences as part of a program designed to create peptides whose helicity could be controlled by photoisomerizable cross-linking reagents (*29*, *30*). In the course of these studies, we found that the mutations introduced had marked effects on the solubility behavior of the peptides. Specifically, it was found that the peptide JRK-{ValAib} was fully soluble at high concentrations in water, whereas JRK-{ValAla} was extremely insoluble in water, methanol, and acetonitrile/water mixtures. We therefore sought to test the mechanism whereby this relatively subtle chemical change (a single CH_3 for H) could have such a dramatic effect.

It should be noted that reducing conditions were used throughout to ensure that there was no possibility of intermolecular disulfide bond formation. In all assays (CD, FTIR, EM, and dye-binding), an excess of DTT was present that ensured that the cysteine residues remained in a reduced state.

The secondary structures of these four peptides were analyzed using both CD in the far-UV region and FTIR spectroscopy in the amide I region (Figures 2 and 3). The amide II region of each spectrum was examined at 1550 cm^{-1} to check that H to D exchange was complete. In every case, there was no measurable amide II peak (unpublished results) indicating that the amide groups of the peptides had exchanged thus simplifying analysis of the amide I region.

Comparing JRK-{AlaAla} with JRK-{AlaAib} in Figure 2A, CD analysis of aqueous solutions of the peptides shows that JRK-{AlaAib} has a mixed random-coil/α-helical type spectrum characterized by minima at 202 and 222 nm, whereas JRK-{AlaAla} has a minimum at 220 nm and maximum at 200 nm characteristic of a β-sheet structure (*31*, *32*).

The FTIR analysis of JRK-{AlaAla} and JRK-{AlaAib} also indicated a distinct difference in secondary structure (Figure 2B). The JRK-{AlaAib} spectrum is dominated by a band at 1643 cm^{-1} indicative of a peptide predominantly in an unordered conformation with the possibility of some α-helical structure, whereas JRK-{AlaAla} has a band at 1617 and 1696 cm^{-1} suggestive of an aggregated β-sheet structure. The sheet may be parallel, as antiparallel β-sheet structure is expected to give amide signals closer to 1625−1640 cm^{-1} (*33*). The peak at 1672−1674 cm^{-1} in each spectrum is attributed to residual trifluoroacetic acid (necessary for the HPLC purification of the peptides) (*33*).

Spectroscopic analysis of the conformations of JRK-{ValAib} and JRK-{ValAla} in aqueous solvent is shown in Figure 3. CD analysis (Figure 3A) and FTIR analysis (Figure 3B) of JRK-{ValAib} both indicate a mixture of random-coil/α-helical structure, similar to that of JRK-{AlaAib}. JRK-{ValAib} was freely soluble in water whereas, in direct contrast, JRK-{ValAla} was extremely

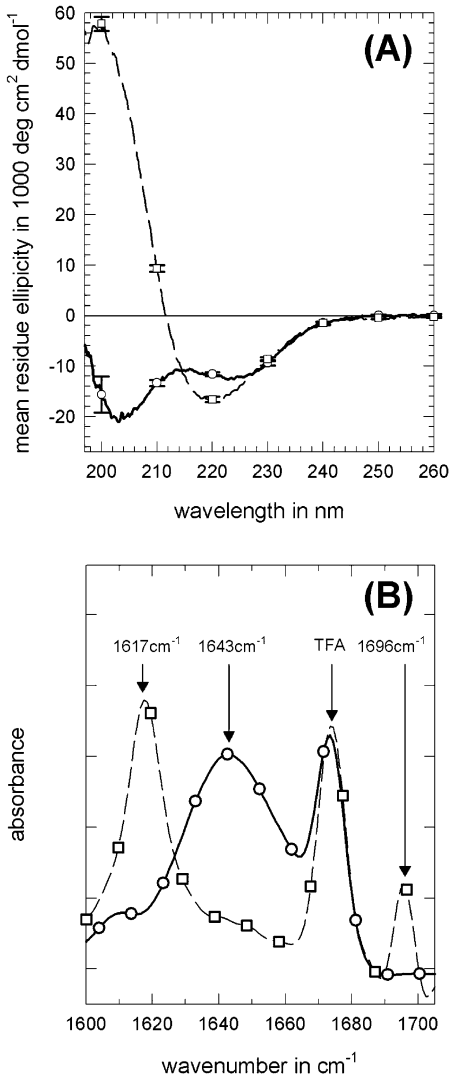

FIGURE 2: CD spectra (A) and FTIR spectra (B) observed for JRK-{AlaAib} and JRK-{AlaAla}. In both cases results for JRK-{AlaAib} are marked by a solid line and open circles (○), whereas JRK-{AlaAla} are shown with dashed lines and squares (□).

insoluble. The resulting suspension yielded an FTIR spectrum, with three peaks in the amide I region: a predominant one at 1618 cm^{-1} indicating a β-sheet, and two weaker ones at 1644 and 1696 cm^{-1} (Figure 3B) indicating some unordered/α-helical structure, in contrast to JRK-{AlaAla}. The insolubility of the peptide complicated CD analysis so that only a qualitative spectrum was obtained (Figure 3A, inset); this too indicated the presence of predominantly β-sheet structure. These results suggest that JRK-{ValAla} aggregates quickly without complete ordering into β-structure. In comparison, the strong β-signal and greater solubility of JRK-{AlaAla} suggested that this peptide may be forming a fibril.

Electron microscopy and dye binding studies were consequently undertaken to examine whether JRK-{AlaAla} was forming fibrils. Figure 4A shows that fibrils are observed by EM for JRK-{AlaAla} after 3 days. The fibrils have a straight morphology typical of the fibrils formed by peptides (*7*, *11*, *34*−*36*). Compared to other images, the fibrils are shorter than might be expected, with the exception of Hughes et al. (*11*) and Goldsbury et al. (*35*) who have reported images of β-amyloid peptide fragments with approximately

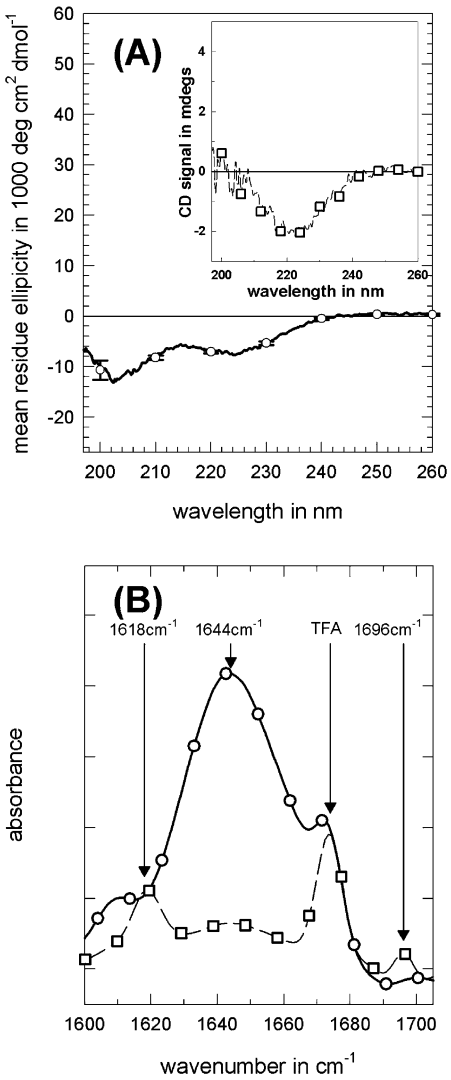

FIGURE 3: CD spectra (A) and FTIR spectra (B) observed for JRK-{ValAib} and JRK-{ValAla}. In both cases results for JRK-{ValAib} are marked by a solid line and open circles, whereas JRK-{ValAla} are shown with dashed lines and squares. Only a qualitative CD analysis (inset) was possible for JRK-{ValAla} because of its low solubility.

the same length. After 18 days, maturation EM shows that the JRK-{AlaAla} fibrils have clumped together forming a mesh-like structure. Such behavior is also typical for fibril forming peptides (*35*). The soluble variant JRK-{AlaAib} was also studied under identical conditions to provide a control for the experiment with the result that no fibrils were observed (Figure 4C).

The results of the EM studies are complemented by dye binding experiments. The binding of the fluorescent dye, ANS, to exposed hydrophobic surfaces results in an increase in the ANS fluorescence intensity as well as a blue shift of the maximum (*25*). Figure 5A shows that just such an effect is found when JRK-{AlaAla} is exposed to ANS, indicating that the dye has bound to the peptide. In contrast, the fluorescence of ANS is not affected by the presence of JRK-{AlaAib} (Figure 5A). This shows that there is no binding between ANS and JRK-{AlaAib} and therefore little or no exposed hydrophobic surfaces on the peptide for the dye to bind. These results can be compared to those of Smith and Radford (*25*) who found that β_2-microglobulin showed no

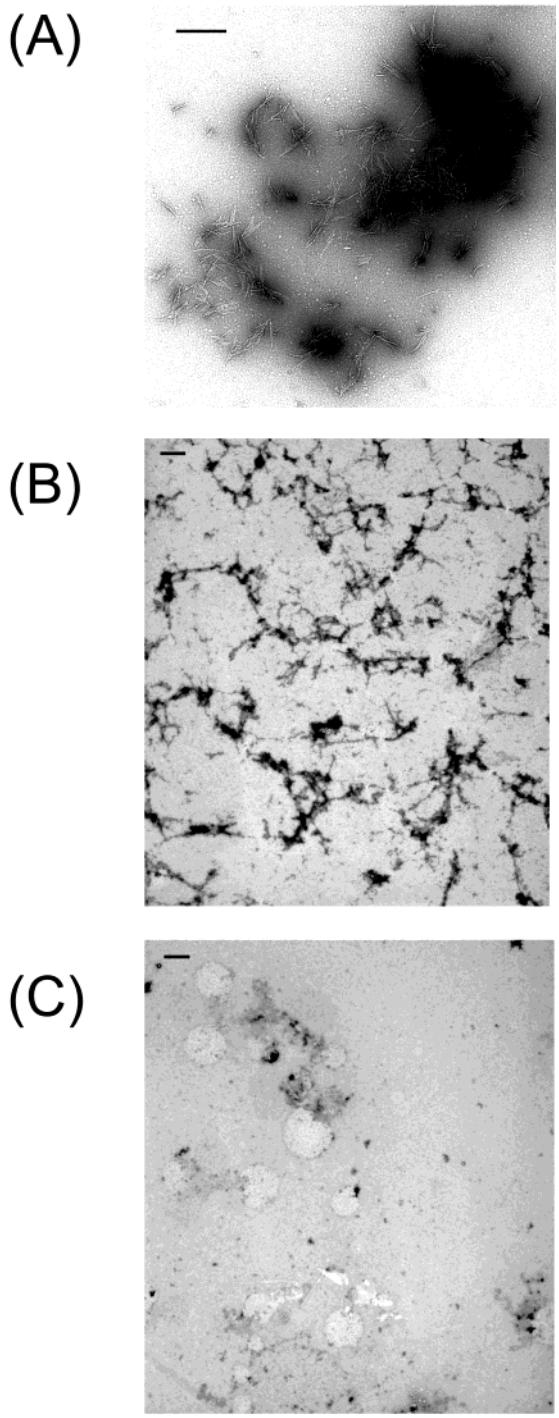

FIGURE 4: Negative stain EM image of the fibrils formed by (A) JRK-{AlaAla} after 3 days maturation of 0.3 mg/mL solution (scale bar of 200 nm). Panel B shows the same sample after 18 days maturation forms a mesh (scale bar of 500 nm). The control experiment using the same concentration of the nonfibril forming peptide JRK-{AlaAib}, panel C, shows no such structures (scale bar of 500 nm).

detectable ANS binding when in a soluble form but bound the dye under conditions where the protein had aggregated.

Thio-T is a dye that is widely used to assay the formation of fibrils both in pathology and in scientific studies. Levine has shown for the Alzheimer $\beta(1-40)$ peptide (*37*) that soluble pentameric/hexameric pre-amyloid complexes do not bind the dye whereas fibrils do. This specificity is not absolute, however, as demonstrated by Carrotta et al. (*38*)

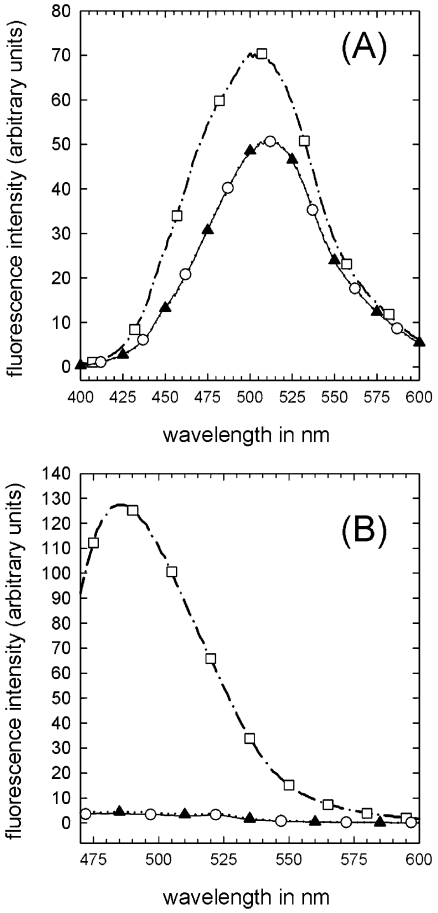

FIGURE 5: Dye binding assays. Fluorescence emission spectra of (A) ANS and (B) Thio-T. In both cases the spectrum of the dye in the absence of peptide is shown by a dotted line and marked by filled triangles (▲). The spectra of the dyes in the presence of JRK-{AlaAib}, marked by a solid line and open circles (○), can be seen to be unaltered. This contrasts with the results for an identical amount of JRK-{AlaAla} marked by a dashed line and squares (□), where in both cases a marked increase in fluorescence was observed.

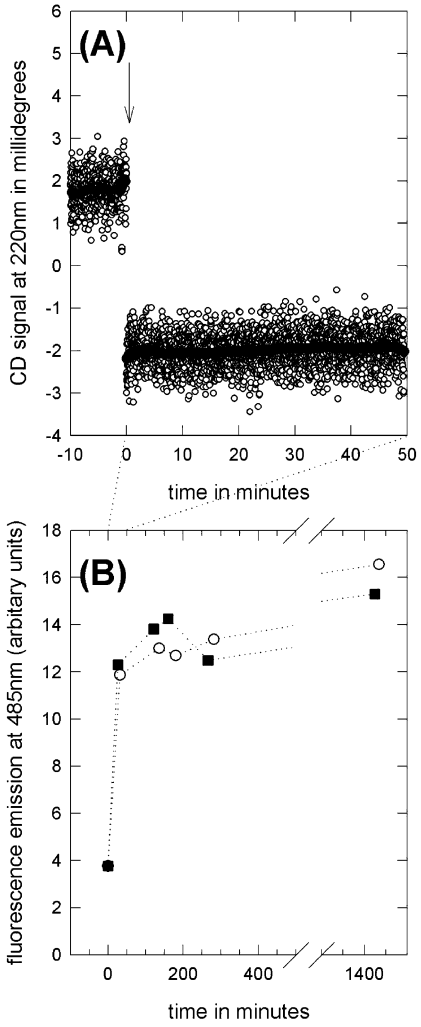

FIGURE 6: How (A) CD and (B) Thio-T fluorescence signals change after JRK-{AlaAib} is dissolved. Both CD and Thio-T signal changes are shown for a peptide concentration of ~15 μM by open circles (○). The fluorescence signal for ~180 μM peptide is shown by filled squares (■) in panel B.

who found that in the heat-induced aggregation of β-lactoglobulin both oligomeric intermediates and the final spherical aggregates bind Thio-T, whereas the monomeric form of the protein does not. It is also possible to produce fibrils that do not bind Thio-T; however, the binding of Thio-T is very strong evidence that a fibril-like aggregate is present (*35*). The results of Thio-T binding assays are shown in Figure 5B. Once again, it is clear that the addition of JRK-{AlaAib} has no measurable effect on the fluorescence of the dye. In contrast, addition of an equivalent amount of JRK-{AlaAla} produces a large increase in fluorescence with a maximum at 485 nm as previously observed for amyloid forms of peptides (*7*) and proteins (*25*), indicating the formation of fibril-like structures.

To further characterize the nature of fibril formation for the time dependence of both CD and Thio-T, fluorescence signals of JRK-{AlaAla} after the peptide was dissolved were examined (Figure 6). It can be seen (Figure 6A) that the appearance of a CD signal characteristic of β-sheet is rapid with no measurable change over 50 min. The Thio-T fluorescence signal in contrast shows an immediate rise followed by a slow increase over many hours (Figure 6B). There appears to be little effect of peptide concentration on the change (Figure 6B). Taken with the EM data (Figure 4), it can be proposed that fibril nucleation is rapid for JRK-{AlaAla} but that there is a slow maturation of the fibrils that then clump together. This is in contrast to fibril formation by amyloid forming proteins where a lag phase is normal, with CD signals characteristic of β-sheet often taking days to appear (*39*). In a recent study, Johansson and co-workers (*40*) show that for short fibril-forming peptides a CD signal characteristic of β-sheet is immediately formed but waited 10 days to take EM data.

Given the evidence that the peptide variants without Aib were forming fibrils, molecular modeling was undertaken to explore possible modes of association of the peptides. Models were produced with the peptide forming a parallel β-sheet based on the indication from FTIR measurements that this is the most likely conformation. Figure 7 shows one possibility for the formation of a β-tape (*41*, *42*) by JRK-{ValAla}. In comparison to models of β-tapes in which strands associate in an antiparallel manner (*41*, *42*), it is necessary to stagger the association to preserve reasonable interactions between charged residues. This also has the effect of improving the packing of bulky residues (V and C) on the hydrophobic face of the tape. It should be noted that, as a parallel β-sheet is normally curved, packing of the

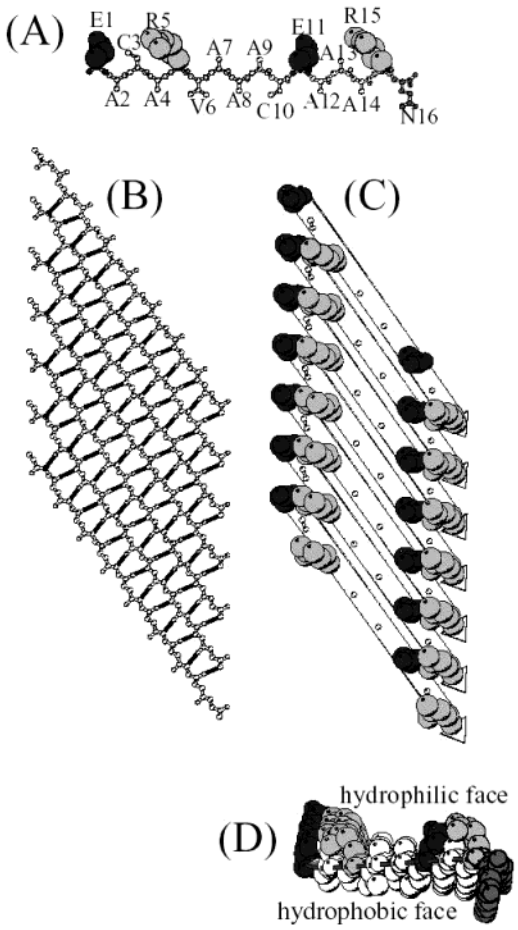

FIGURE 7: Model for the formation of a β-tape (*41*, *42*) by JRK-{ValAla}. (A) A view from the side of JRK-{ValAla} modeled as a β-strand. A number of strands could associate together to form a parallel β-sheet. (B) shows the main chain atoms of such a sheet as balls and sticks and the hydrogen bonds as thick black lines. (C) The possibility of stabilization of such a sheet by salt bridges being formed by glutamic acid (dark gray spheres) and arginine (light gray spheres) residues interacting from adjacent strands. A side view of such a tape—panel D—shows that it would present a hydrophilic face opposite a reasonably flat hydrophobic face (which could then associate). The model tape has a width of approximately 34 Å and a height of 12 Å. Each strand (length 54 Å) has an angle of approximately 50° relative to the tape direction.

hydrophobic faces between adjacent tapes could be more difficult to achieve in comparison to antiparallel models. In addition, the model only presents one possible way in which formation of such a sheet could occur. It would clearly be possible to form more extended sheets, and a mixture of parallel and antiparallel associations between strands would also be possible.

DISCUSSION

These results clearly indicate that the Ala → Aib substitution can have a dramatic effect on the conformational behavior of these peptides in an aqueous environment. The single H → CH_3 replacement evidently interferes with sheet formation preventing the formation of fibrils for JRK-{AlaAla} or rapid peptide aggregation and insolubility with JRK-{ValAla}. A similar effect has also been observed in peptides with *N*-methyl amino acids where a methyl group is substituted for the hydrogen atom of the main chain nitrogen (*11*). However, the conformational properties of Aib are quite distinct from *N*-methyl amino acids that are locked in a β-conformation (*12*, *43*). The second α-methyl group of Aib is known to create local steric interactions that restrict backbone torsion angles φ and ψ, to a small region close to α and 3_{10}-helical values (*44*, *45*). X-ray crystal structures (*46*−*48*) and solution NMR structures (*47*, *49*) of a variety of Aib-containing peptides and proteins revealed a tendency for helix formation—either 3_{10}-helix or α-helix—depending on the length of the peptide, type of solvent, and also on the number of Aib residues present (*17*, *46*, *50*, *51*). However, it is noteworthy that the helix propensity of Aib has been found to be similar to alanine (*16*). Results presented here lead to a view that Aib should be regarded much more as a sheet disrupter than as a helix promoter.

Since this series of peptides was originally derived from sequences known to form monomeric helices in water, our finding of β-sheet structure and peptide aggregation was initially somewhat surprising. The unintentional formation of fibrils can be explained by the injudicious positioning of all charged amino acids in the odd numbered positions in the amino acid sequence. It is interesting to note that fibril formation may be a common misfold in many proteins and peptide fragments: Kallijärvi et al. (*52*) have recently shown how it is possible to identify amyloid forming fragments using physiochemical considerations.

As noted above, Aib occurs commonly in peptaibol antibiotics (*14*). Because of their mode of action in lipid bilayers, these peptides must be predominately hydrophobic, yet pass through an aqueous phase. In a study on fragments of the integral membrane protein bacteriorhodopsin, Engleman and co-workers (*53*) found that helix G in isolation forms a very stable misfold with a predominately β-sheet character. This showed the potential for such hydrophobic sequences to form misfolded aggregates and led to the hypothesis that chaperones may be needed to ensure the correct folding of integral membrane proteins (*53*). Since peptaibol antibiotics are secreted peptides, a chaperonin-based mechanism to prevent misfolding would not be possible. From the results presented here, it is likely that the presence of Aib helps to ensure that the peptaibol antibiotics do not misfold, either in the aqueous phase or during lipid insertion. In support of this idea is the observation of Spach and co-workers that an alamethicin derivative in which Aib residues were replaced by Ala had a great tendency to convert into an aggregated β-structure and was unable to form functional ion channels (*54*).

The results presented here show that Aib provides an alternative to proline (*7*−*9*), D-amino acid (*7*, *10*), or *N*-methylated amino acid (*11*) substitution in producing peptide variants that have a lower tendency to form fibril aggregates. The dramatic changes in conformational properties observed for a single Aib substitution suggest that the disruptive effect is at least as strong as that of other changes. Furthermore, Aib substitution could be useful where it is desired to allow helix formation in the final product, in contrast to the other modifications described above. A particular use could be in structural studies of hydrophobic peptides by NMR where the high concentrations needed can lead to aggregation (*55*). In this context, it is interesting to note that an alternative way to stop fibril formation is provided by cross-linking (*56*). We have recently shown (*56*) that the JRK-{AlaAla} peptide is fully soluble and shows

no tendency to aggregate once the two cysteine residues (Figure 1) have been cross-linked using an azobenzene derivative.

Recent work on Alzheimer's β-peptide has indicated that oxidative damage may be important in toxicity (*57*, *58*). However, it is unclear whether the damage occurs when the peptide is in a sheet (*57*) or a helical (*58*) conformation. Butterfield et al. (*58*) used proline substitution as a helix breaking method to test the mechanism of action. However, they noted that this substitution also disrupted the peptides' ability to form fibrils (*58*). We propose that Aib substitution provides a useful means to examine the importance of different conformations in the mechanism of action of fibril-forming peptides.

ACKNOWLEDGMENT

We would like to thank Lesley Tomkins of The University of Birmingham Electron Microscopy Centre for help with EM imaging.

REFERENCES

1. Kelly, J. W. (2002) *Nat. Struct. Biol. 9*, 323−325.
2. Prusiner, S. B. (1998) *Proc. Natl. Acad. Sci. U.S.A. 95*, 13363−13383.
3. Bucciantini, M., Giannoni, E., Chiti, F., Baroni, F., Formigli, L., Zurdo, J. S., Taddei, N., Ramponi, G., Dobson, C. M., and Stefani, M. (2002) *Nature 416*, 507−511.
4. Walsh, D. M., Klyubin, I., Fadeeva, J. V., Cullen, W. K., Anwyl, R., Wolfe, M. S., Rowan, M. J., and Selkoe, D. J. (2002) *Nature 416*, 535−539.
5. Srisailam, S., Kumar, T. K. S., Srimathi, T., and Yu, C. (2002) *J. Am. Chem. Soc. 124*, 1884−1888.
6. Taddei, N., Capanni, C., Chiti, F., Stefani, M., Dobson, C. M., and Ramponi, G. (2001) *J. Biol. Chem. 276*, 37149−37154.
7. Soto, C., Kindy, M. S., Baumann, M., and Frangione, B. (1996) *Biochem. Biophys. Res. Commun. 226*, 672−680.
8. Soto, C., Kascsak, R. J., Saborio, G. P., Aucouturier, P., Wisniewski, T., Prelli, F., Kascsak, R., Mendez, E., Harris, D. A., Ironside, J., Tagliavini, F., Carp, R. I., and Frangione, B. (2000) *Lancet 355*, 192−197.
9. Wood, S. J., Wetzel, R., Martin, J. D., and Hurle, M. R. (1995) *Biochemistry 34*, 724−730.
10. Kaneko, I., Morimoto, K., and Kubo, T. (2001) *Neuroscience 104*, 1003−1011.
11. Hughes, E., Burke, R. M., and Doig, A. J. (2000) *J. Biol. Chem. 275*, 25109−25115.
12. Doig, A. J. (1997) *Chem. Commun.* 2153−2154.
13. Woolley, G. A., and Wallace, B. A. (1992) *J. Membr. Biol. 129*, 109−136.
14. Chugh, J. K., and Wallace, B. A. (2001) *Biochem. Soc. Trans. 29*, 565−570.
15. Toniolo, C., Crisma, M., Formaggio, F., Valle, G., Cavicchioni, G., Precigoux, G., Aubry, A., and Kamphuis, J. (1993) *Biopolymers 33*, 1061−1072.
16. O'Neil, K. T., and deGrado, W. F. (1990) *Science 250*, 646−651.
17. Kaul, R., and Balaram, P. (1999) *Bioorg. Med. Chem. 7*, 105−117.
18. Moretto, V., Crisma, M., Bonora, G. M., Toniolo, C., Balaram, H., and Balaram, P. (1989) *Macromolecules 22*, 2939−2944.
19. Narita, M., Chen, J. Y., Sato, H., and Kim, Y. (1985) *Bull. Chem. Soc. Jpn. 58*, 2494−2501.
20. Kaduk, C., Wenschuh, H., Beyermann, M., Forner, K., Carpino, L. A., and Bienert, M. (1996) *Lett. Peptide Sci. 2*, 285−288.
21. Kauppinen, J. K., Moffatt, D. J., Mantsch, H. H., and Cameron, D. G. (1981) *Appl. Spectrosc. 35*, 271−276.
22. Lesk, A. M. (2001) *Introduction to Protein Architecture*, Oxford University Press, Oxford.
23. Cornell, W. D., Cieplak, P., Bayly, C. I., Gould, I. R., Merz, K. M., Ferguson, D. M., Spellmeyer, D. C., Fox, T., Caldwell, J. W., and Kollman, P. A. (1995) *J. Am. Chem. Soc. 117*, 5179−5197.
24. Kraulis, P. J. (1991) *J. Appl. Crystallogr. 24*, 946−950.
25. Smith, D. P., and Radford, S. E. (2001) *Protein Sci. 10*, 1775−1784.
26. Merutka, G., and Stellwagen, E. (1990) *Biochemistry 29*, 894−898.
27. Merutka, G., Shalongo, W., and Stellwagen, E. (1991) *Biochemistry 30*, 4245−4248.
28. Marqusee, S., Robbins, V. H., and Baldwin, R. L. (1989) *Proc. Natl. Acad. Sci. U.S.A. 86*, 5286−5290.
29. Kumita, J. R., Smart, O. S., and Woolley, G. A. (2000) *Proc. Natl. Acad. Sci. U.S.A. 97*, 3803−3808.
30. Flint, D. G., Kumita, J. R., Smart, O. S., and Woolley, G. A. (2002) *Chem. Biol. 9*, 391−397.
31. Brahms, S., and Brahms, J. (1980) *J. Mol. Biol. 138*, 149−178.
32. Johnson, W. C. (1990) *Proteins 7*, 205−214.
33. Haris, P. I., and Chapman, D. (1995) *Biopolymers 37*, 251−263.
34. Takahashi, Y., Ueno, A., and Mihara, H. (1999) *Bioorg. Med. Chem. 7*, 177−185.
35. Goldsbury, C. S., Wirtz, S., Muller, S. A., Sunderji, S., Wicki, P., Aebi, U., and Frey, P. (2000) *J. Struct. Biol. 130*, 217−231.
36. Aggeli, A., Nyrkova, I. A., Bell, M., Harding, R., Carrick, L., McLeish, T. C. B., Semenov, A. N., and Boden, N. (2001) *Proc. Natl. Acad. Sci. U.S.A. 98*, 11857−11862.
37. Levine, H. (1995) *Neurobiol. Aging 16*, 755−764.
38. Carrotta, R., Bauer, R., Waninge, R., and Rischel, C. (2001) *Protein Sci. 10*, 1312−1318.
39. Fezoui, Y., and Teplow, D. B. (2002) *J. Biol. Chem. 277*, 36948−36954.
40. Tjernberg, L., Hosia, W., Bark, N., Thyberg, J., and Johansson, J. (2002) *J. Biol. Chem. 277*, 43243−43246.
41. Cerpa, R., Cohen, F. E., and Kuntz, I. D. (1996) *Fold. Des. 1*, 91−101.
42. Aggeli, A., Bell, M., Boden, N., Keen, J. N., Knowles, P. F., McLeish, T. C. B., Pitkeathly, M., and Radford, S. E. (1997) *Nature 386*, 259−262.
43. Manavalan, P., and Momany, F. A. (1980) *Biopolymers 19*, 1943−1973.
44. Burgess, A. W., and Leach, S. J. (1973) *Biopolymers 12*, 2599−2605.
45. Paterson, Y., Rumsey, S. M., Benedetti, E., Nemethy, G., and Scheraga, H. A. (1981) *J. Am. Chem. Soc. 103*, 2947−2955.
46. Marshall, G. R., Hodgkin, E. E., Langs, D. A., Smith, G. D., Zabrocki, J., and Leplawy, M. T. (1990) *Proc. Natl. Acad. Sci. U.S.A. 87*, 487−491.
47. Nagaraj, R., Shamala, N., and Balaram, P. (1979) *J. Am. Chem. Soc. 101*, 16−20.
48. Karle, I. L., Das, C., and Balaram, P. (2000) *Proc. Natl. Acad. Sci. U.S.A. 97*, 3034−3037.
49. Bellanda, M., Peggion, E., Burgi, R., van Gunsteren, W., and Mammi, S. (2001) *J. Pept. Res. 57*, 97−106.
50. De Filippis, V., De Antoni, F., Frigo, M., de Laureto, P. P., and Fontana, A. (1998) *Biochemistry 37*, 1686−1696.
51. Ratnaparkhi, G. S., Awasthi, S. K., Rani, P., Balaram, P., and Varadarajan, R. (2000) *Protein Eng. 13*, 697−702.
52. Kallijärvi, J., Haltia, M., and Baumann, M. H. (2001) *Biochemistry 40*, 10032−10037.
53. Hunt, J. F., Earnest, T. N., Bousché, O., Kalghatgi, K., Reilly, K., Horváth, C., Rothschild, K. J., and Engelman, D. M. (1997) *Biochemistry 36*, 15156−15176.
54. Molle, G., Duclohier, H., Dugast, J. Y., and Spach, G. (1989) *Biopolymers 28*, 273−283.
55. Sailer, M., Helms, G. L., Henkel, T., Niemczura, W. P., Stiles, M. E., and Vederas, J. C. (1993) *Biochemistry 32*, 310−318.
56. Kumita, J. R., Flint, D. G., Smart, O. S., and Woolley, G. A. (2002) *Protein Eng. 15*, 561−569.
57. Rauk, A., Armstrong, D. A., and Fairlie, D. P. (2000) *J. Am. Chem. Soc. 122*, 9761−9767.
58. Kanski, J., Aksenova, M., Schoneich, C., and Butterfield, D. A. (2002) *Free Rad. Biol. Med. 32*, 1205−1211.

BI026856T